Mathematical Modelling of Engineering Problems
Vol. 12, No. 6, June, 2025, pp. 2031-2044
Journal homepage: http://iieta.org/journals/mmep

Experimental and Finite Element Investigation of the Free Vibration Behavior for Functionally Graded Plate

Raghad Azeez Neamah, Hyder M. Abdul Hussein, Alaa M.H. Aljassani*, Luay S. Al-Ansari

Mechanical Engineering Department, Faculty of Engineering, University of Kufa, Najaf 54001, Iraq

Corresponding Author Email: alaa.aljasani@uokufa.edu.iq

https://doi.org/10.18280/mmep.120618

Received: 17 December 2024
Revised: 25 February 2025
Accepted: 21 March 2025
Available online: 30 June 2025

Keywords:
FG-plate, vibration analysis, natural frequency, finite element method, material index, power-law model

ABSTRACT

Functionally graded materials (FGMs) are developed to meet the evolving demands of the advanced technology in several engineering applications. There are many numerical and experimental techniques in the literature to emulate the FGM. This paper introduces a novel experimental technique to fabricate functionally graded (FG) plate made from polyester resin and silica powder. The power law model is utilized to represent the material distribution along the thickness of the FG plate. The fundamental natural frequency of the FG plate for different material indices are measured experimentally using the novel experimental method. In addition, a finite element method is utilized to simulate the free vibration of the FG plate using ANSYS software. The numerical results of ANSYS program are compared with the experimental one and the results indicated a very good agreement. Furthermore, a comparison is made with the available literatures as verification. The effect of various parameters such as material index, modular ratio, length-to-thickness ratio and supporting type on the first five natural frequencies of the FG plate are investigated. The results indicated that the modular ratio has a great effect on the natural frequencies of FG plate for different supporting types. Also, the natural frequencies decrease as the ratio of (L/h) increase.

1. INTRODUCTION

The structural mechanics has seen a notable development in latest years, because of the increasing demand for high-performance and lightweight materials in several application such as spacecraft, bio-mechanics, vehicles, nuclear, and civil engineering applications [1-3]. Functionally graded materials (FGMs) introduced as a promising solution to address the complex structural and thermal challenges encountered in various engineering systems. Nowadays, FGMs have become one of the intelligent materials as well as, from the structure's upper to lower surfaces, it offered a constant change in characteristics of material [3]. FGMs can be defined as "non-homogeneous composite materials in which the composition varies continuously and smoothly in a specific direction, such as along the length or thickness" [3]. FGMs are composed of two or more components and proven to be very effective in structural design, overcoming the performance of traditional homogenous and composite materials [3]. Because of its high applicability FGMs, several researches investigated the material properties and mechanical behavior of these materials depending on various theories [4-8].

On the other hand, the vibration of functionally graded (FG)-plate took a considerable area in the academic community for their wide applications. In aerospace usually used as barrier thermal isolation for parts with extreme temperature gradients. Also, they utilized in landing gears, engine mount, and suspension systems for their good vibration isolation. For example, using appropriate displacement functions for both forced and free vibrations, Vel and Batra [9] enhanced a 3-D precise solution behavior to employed simply supported (SS) for rectangular thin and thick FG-plate and boundary condition for appropriate displacement functions. The first, third, and classical theories of shear deformation were used to compute natural frequencies, displacements, and stresses. The effective properties were computed at all point along the plate's thickness using Mori-Tanaka or self-consistent techniques. Furthermore, they applied a power law model to represented the variation in material characteristics along the plate's thickness. Altenbach and Eremeyev [10], calculated natural oscillations of FGM-plates taking into consideration the effects of the rotatory inertia and the transverse shear stiffness. Natarajan et al. [11], utilized the extended finite element technique to analysis free transverse vibration behavior of cracked FG-plate. The impact of material index and fracture dimensions (location, length, and direction) were investigated using his model, thickness of plate and presence of multiple cracks on natural frequency and mode shape of rectangular and square FG-plate with the boundary condition of simply supported and clamped. Janghorban and Rostamsowlat [12], performed the free vibration behavior of FG-plate containing non-circular and multi circular interruptions employing finite element mechanism. Considered the effects of (a) number, size, and location of

cutouts, (b) supporting types, and (c) shape of FG-plate (rectangular, skew, trapezoidal, and circular) on the FG-plate natural frequency. Lei et al. [13] examined the vibration behavior of FG-plate reinforced by the carbon nanotubes with a single wall with various distribution patterns of uniaxial aligned single wall carbon nano-tubes (SWCNTs) using the kp-Ritz method. Linear volume fraction utilized several distributions of carbon nanotubes, employing functionally graded-carbon nanotubes reinforced composites (FG-CNTRCs) to modify the characteristics throughout the thickness. The study investigated how natural frequencies and mode shapes were affected by factors such as temperature changes, boundary conditions. Sharma et al. [14] applied the finite element technique to analyze the free vibration behavior of FG-plate with multiple circular cutouts describing the material's properties using power law model characteristics along the thickness of the plate. Due to material index, thickness ratio and supporting types were studied the variation of natural frequency.

Gupta et al. [15] examined the free vibration behavior of FG-plates which has been used, the theory of higher-order shear deformation in the type of simply supported was applied to an elastic base. Pasternak model utilized to simulate the foundation with power law approach to model the characteristics of the material throughout its thickness of FG-plate. The study examined how the distribution index, FG-plate dimensions, and two Pasternak elastic foundation parameters affected the natural frequency variation. Also, Song et al. [16] applied 1st-order theory of shear deformation and modified Halpin-Tsai model to examine the FG-plate vibration behavior, both forced and free made by multilayer graphene nano-platelet (GPL) polymer composite. Simply supported FG-plates and natural frequency and reactivity under dynamic loads were determined using the Navier solution method. Conversely, Ghasabí [17] investigated how the length of the dimensionless plate, the material index, and the nonlocal parameter ratio affected the natural frequency by using a nonlocal elasticity-based technique to analyze the free vibration behavior of a nano-plate created via FGM. Using the variational approach and Hamilton's principle to obtain the equations and boundary conditions, then applied the extended strategy of differential quadrature to solve the resulting governing equations. Akbas [18] derived the static and free vibration equations of a porous FG-plat using the concepts of Hamilton's principle and shear deformation plates of the first order. Furthermore, the plate situation was applied simply supported in both ends of a plate and solved by the Navier method.

Hien and Lam [19] used a power-law model to describe the change in material characteristics over the thickness of the FG-plate and examined the dynamical response of a rectangular FG-plate lying on a viscoelastic foundation under changing loads. The transient responses of simply supported FG-plates were used to computed state-space techniques, higher-order shear deformation, and Hamilton's principle.

Also, Sharma et al. [20] used 4-nodes shell element and power law equation to simulate the vibration and harmonic behaviors of FG-plates made by (Aluminum-Alumina, Ti–6Al–4V-Aluminum oxide, Aluminum-Zirconia, and SUS304/Si_3N_4). The study focuses on verifying influence of material types, damping on natural frequency, supporting types, distribution index and harmonic response of FG-plates. Nguyen et al. [21], using the analysis of extended isogeometric (XIGA) to characterize the displacement field of the FG-plate and the approach of simplified strain gradient. The vibration behavior of cracked FG-microplates was examined using the refined plate theory, which comprises four unknowns.

In order to examine the nonlinear dynamic response of FG-plate under external dynamic loads while taking into account the third order shear deformation plate kinematics (TSDT), Bourihane et al. [22], used a Methodology of high-order implicit based on the asymptotic numerical method (ANM) techniques. To develop a finite element model applied a four-node quadrilateral element (7 degrees of freedom) without used homogenization techniques. Hadji and Avcar [23] applied hyperbolic shear displacement theory along with Hamilton's principle to explore the free vibration of a square porous FG sandwich plate featuring an isotropic homogeneous core, while examining various support configurations. Their investigated how factors such as the porosity index, porosity distribution function, layer arrangement, side thickness ratio, and support types influenced the vibrational behavior of the sandwich porous FG plate. Permoon and Farsadi [24] employed fractional theory to model and investigate the free vibration and damping behavior of a three-layer sandwich plate with a viscoelastic core. The Rayleigh-Ritz approach used to solve the governing equation of vibration after applying Lagrange's method to derive it.

An accurate high-order shear deformation theory issue of sandwich FG-plate resting on a viscoelastic foundation under a hygrothermal environment load was used by Zaitoun et al. [25], to investigate the free vibration utilizing Hamilton's principle. sandwich FG-plate density, thickness, damping constant, aspect ratio, temperature, and moisture were studied. The finite element approach was used by Narayanan et al. [26] to study the vibration responses in both forced and free vibration of the FG-plate using Abaqus CAE (S8R5 shell elements). The FG-plate's center receives a harmonic force with a sine function, while the top and center get impulse forces in a rectangle, triangle, and half-cycle sine configuration. The suggested method developed a good acceptance with the existing literature. Cho [7] carried out multiple levels' models developed from the 3D elasticity and the 2-D natural element approach to numerically study the free vibration problem of the sandwich FG plate of a homogenous center. It was discovered that the kind of material that made up the center, the index of volume fraction, the relative thickness and location of the center layer, and the plate aspect ratio all had a substantial impact on the calibrated fundamental frequency. Moreover, Kumar et al. [8] used a non-polynomial hyperbolic based theory that assumed an exponential function for changing material characteristics throughout the plate's thickness to study the free vibration issue of a rectangular tapered FG-plate sitting on an elastic basis. The model was constructed and solved using the variational principle and Galerkin's approach, yielding the impacts of foundation stiffness, span ratio, width to height ratio, and taper ratio supporting types on the frequency of rectangular tapered FG-plate. Li et al. [27] gave a mathematical solution for the sandwich FG-plate free vibration problem by applied a theory of equivalent-single-layer plate and accounting of the effect of thermal environment. Equations of motion for two distinct kinds of sandwich FG-plates were developed by Hamilton's principle and subsequently solved using the Navier theory.

Vu and Tran [28] investigated the effects of sandwich plate

auxetic core and FGM piezoelectric face sheet on free vibration. Refined plate approach of four-variable shear deformation used improved a unique model, and the pb2-Ritz technique. Geometric characteristics, electrical boundary conditions, volume fraction indices, and reinforcing stiffeners are also examined in relation to the vibration response. Hadji et al. [29] carried out the buckling test assumed two sandwich types: FG skins with hard and soft cores, and examined the free vibration of sandwich FG-plate with various supporting types. To construct the current model, Hamilton's principal equations and refined plate models were used.

In this work, a new experimental technique is used to fabricate FG-plate using polyester resin and silica powder (SiO_2). The new technique is to acquire the experimental results of tensile test for seven specimens of polyester-silica composite materials with volume fraction of silica varying from (0-0.3). The power law equation is adopted to fabricate and simulate the FG-plates. Three specimens of FG-plate are fabricated assuming three material indices m=1/2, 1 and 5. An appropriate rig and instruments were used to test the fundamental natural frequency of fabricated FG-plates under clamped-free-free-free conditions (CFFF) experimentally. Three material indices (m=1/2, 1, and 5) were used to build the FE model, and the FE findings were compared with the experimental results of CFFF FG-plates. The ANSYS results were compared with previously published research as a verification of the finite element model. Finally, a numerical investigation is conducted to further study the effects of the following factors: modular ratio, material index, (L/h) ratio, mode number, and supporting type on the natural frequencies of FG-plates.

2. MATERIALS AND METHOD

(a) Resin of polyester (Fiber risen)

(b) Powder of silica (SiO_2)

Figure 1. Elements used to manufacture FG-plate in this work

Table 1. Properties of polyester resin and silica powder [30]

No.	Materials	Young's Modulus (Pa.)	Poisson's Ratio	Density (kg/m^3)
1	Polyester Resin	$2.5*10^9$	0.3	1023
2	Silica Powder	$66.3*10^9$	0.15	2330

2.1 Material

In this paper, two materials types are used to manufacture composite specimens; Polyester resin serves as a matrix material and silica (SiO_2) as a reinforcing material. As a liquid matrix, fiber risen, a well-known polyester resin is used as shown in Figure 1(a). It can be solidified by adding a hardener at a ratio 1:100, and has a lower viscosity than other thermosets. Among the most complicated and intricate material kinds are silicon dioxide (SiO_2), sometimes referred to as silica. It can be appearing naturally in variety of minerals and manufactured synthetically. To prepare polymer composite materials, SiO_2 is highly utilized as fillers because of its fracture toughness, high strength, wear resistance, and high specific surface area. Additionally, it is excellent thermal isolator. Also, it can be a very good electrical insulator, which makes it ideal for isolating the transistors as well as the integrated circuits. Figure 1(b) illustrates the silica particles. The material properties of silica and polyester are listed in Table 1.

2.2 Dies tensile test specimens' preparation

Each of the dies used to create the specimens has three layers and is composed of acrylic. With dimensions of 0.6 m width, 0.22 m length, and 0.01 m thickness, the first layer serves as a cover for the second layer, while the second layer features grooves of the specimen shape used for testing on the third layer, which was utilized as a base to seal mixture leakage (see Figure 2). In order to produce composite samples that meet the international standard specimens (ISS), the die was made using a CNC laser cut machine and roots.

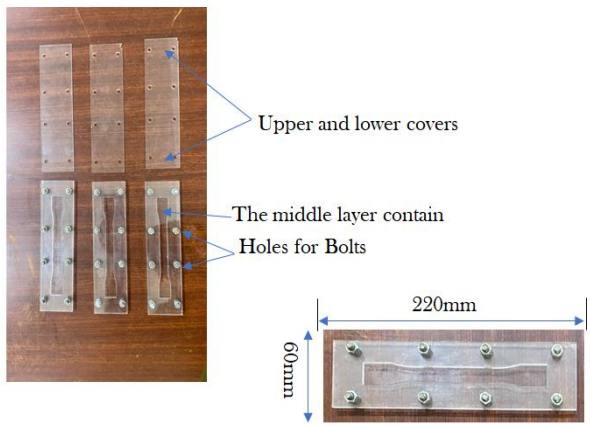

Figure 2. Tensile test die

2.3 Fabrication of tensile test specimens

In order to investigate how the volume percentage of silica affects the composite material of Young's modulus, homogeneous tensile specimens are made using seven different silica volume fractions. Once the acrylic dies for the

tensile test specimens have been prepared using the volume fractions listed in Table 2, the polyester resin and silica powder are thoroughly mixed using a mechanical mixer, taking ample time for each mixing. Then the mixture is poured into the molds and the hardener is added (see Figure 3).

Table 2. Volume fractions of silica and polyester resin used to manufacture tensile test specimens

No.	Silica Volume Fraction	Polyester Resin Volume Fraction	No. of Specimens
1	0	1	3
2	0.05	0.95	3
3	0.1	0.9	3
4	0.15	0.85	3
5	0.2	0.8	3
6	0.25	0.75	3
7	0.3	0.7	3

V_{Silica}=0.05 V_{Silica}=0.1 V_{Silica}=0.15

Figure 3. Homogenous tensile test specimens

2.4 Tensile test experiments

The Young's modulus of the twenty-one homogeneous composite materials samples with ASTM D638 specifications is determined by testing. Table 3 lists the tested specimens' Young's modulus. Figure 4 plots the results to determine an equation that describes how the Young's modulus varies with regard to the volume fraction of silica powder (see Eq. (1)).

$$E(V_f) = 1066 * (V_f)^4 - 904.88 * (V_f)^3 + 208.09\,(V_f)^2 + 2.944 * V_f + 2.5032 \quad (1)$$

Table 3. Experimental results of Young's modulus of polyester- silica powder composite materials vs. V_f of silica powder

No.	Polyester Resin Volume Fraction (V_m)	V_f of Silica Powder (V_f)	E of Composite (GPa)
1	1	0	2.5
2	0.95	0.05	3.08
3	0.9	0.1	4.0478
3	0.85	0.15	5.1392
4	0.8	0.2	5.8671
5	0.75	0.25	6.2725
6	0.7	0.3	6.9592

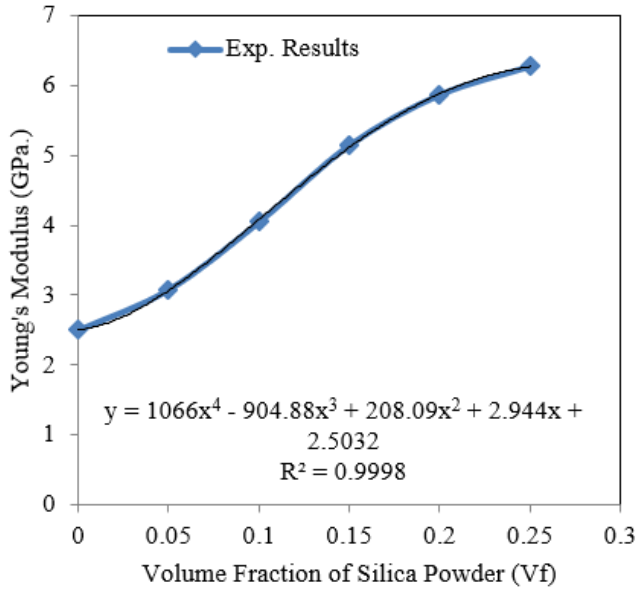

Figure 4. E of composite materials vs. V_f of (SiO_2) particles

2.5 Fabrication of FG-plate for vibration test

The FG-plate's upper material is a composite with a volume proportion of silica powder equal to 0.3, while the bottom material is made of pure polyester according to the power law approximation that describes the properties of material along the plate's thickness. The sample's thickness is divided into five layers in the FGM experimental model, and each layer has consistent properties of material (V_f fraction of silica powder). The Young's modulus of every layer is computed to make use of the following formula to get the necessary V_f of silica powder:

$$E(z) = (E_2 - E_1)\left(\frac{z}{h} + 0.5\right)^m + E_1 \quad (2)$$

where, $E(z)$ represents the Young's modulus at any given location along the FG-plate's thickness (h). The Young's modulus at the FG-plate's top and bottom surfaces is denoted by $E1$ and $E2$, respectively. The power law or distribution index is denoted by m.

To fabricate the FG-plate with power law indices of 1/2, 1, and 5, the following steps were followed:

(a) The bottom material of the FG-plate is the pure polyester while the top material of the FG-plate is the composite material when the volume fraction of silica powder is 0.3. These materials are used in Eq. (2) to calculate the Young's modulus of six points along the thickness of FG-plate (upper, lower and 4 internal points) (see Figure 5).

(b) The following formula is used to determine a layer's Young's modulus:

$$E_{layer\ i} = \frac{\left(E_{point\ i+1} - E_{point\ i}\right)}{2} \quad (3)$$

(c) Using Eq. (1) to calculate the volume fraction of silica powder at each layer for any power law index. Tables 4-6 list the volume fraction of silica powder in each layer where the power law index is 1/2, 1, and 5, respectively.

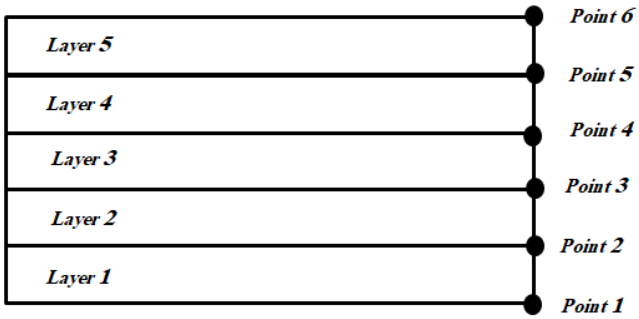

Figure 5. Number of layers and points along thickness of FG-plate

Table 4. Silica powder volume fraction and Young's modulus for the 5 layers (index of power law (m)=1/2)

No.	$E_c=E_{top}$	$E_m=E_{bottom}$	Calculated V_f	E_{layer}
1	6.9588	2.5	0.07	3.497
2	6.9588	2.5	0.12	4.907
3	6.9588	2.5	0.15	5.637
4	6.9588	2.5	0.18	6.221
5	6.9588	2.5	0.22	6.7238

Table 5. Silica powder volume fraction and Young's modulus for the 5 layers (index of power law (m)=1)

No.	$E_c=E_{top}$	$E_m=E_{bottom}$	Calculated V_f	E_{layer}
1	6.9588	2.5	0.05	2.9428
2	6.9588	2.5	0.092	3.8579
3	6.9588	2.5	0.13	4.7387
4	6.9588	2.5	0.18	5.6294
5	6.9588	2.5	0.275	6.5203

Table 6. Silica powder volume fraction and Young's modulus for the 5 layers (index of power law (m)=5)

No.	$E_c=E_{top}$	$E_m=E_{bottom}$	Calculated V_f	E_{layer}
1	6.9588	2.5	0	2.5
2	6.9588	2.5	0.001	2.51
3	6.9588	2.5	0.03	2.6407
4	6.9588	2.5	0.065	3.2404
5	6.9588	2.5	0.145	5.0484

2.6 Vibration of FG-plate

Examining the plate's fundamental natural frequency using the signal data collected is compromised by the vibration test. This test uses FG-plates with the following dimensions: L=50 cm, W=13 cm, and Thickness=2 cm. The boundary condition is cantilevering supported (CFFF).

The flowchart for the vibration structure rig test is displayed in Figure 6. The plate sample that was analyzed to determine the fundamental natural frequency is shown in Figure 7.

The rig contains the following parts:

1). The Rig structure: Used to fix the FG-plate sample on it with support parts for fixing.

2). Impact hammer: The model (086C03) (PCB Piezotronics vibration division) is utilized; the hammer mass (0.16 kg), excitation voltage (20-30 VDC), resonance frequency (≥22 kHz), measurement range (2224 N), and constant current excitation (2×10^{-3}-20×10^{-3} A) are all included.

3). Accelerometer: The model used is SN 151779.

4). Amplifier: The used model is 480E09.

5). Digital data storage oscilloscope; the used model is ADS 1202CL+ with serial No. is 01020200300012, FFT spectrum analysis, the two input channels, the maximum frequency (200 MHz), and the maximum sample r/s (500 MSa/s).

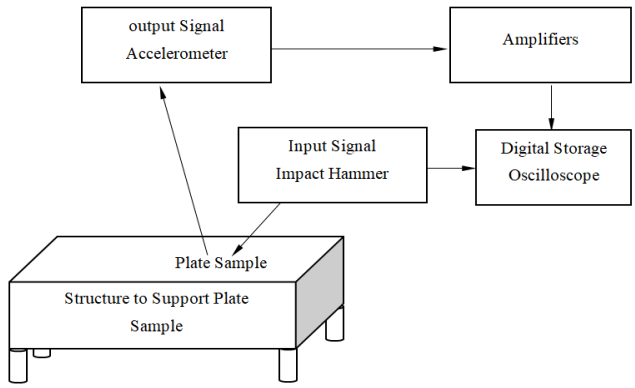

Figure 6. Vibration rig flowchart

Figure 7. Vibration test machine of cantilever FG-plate

3. FINITE ELEMENT SIMULATION

In this work, ANSYS Software is used to apply the method of finite element method (FEM) for simulating together with analyzing the free vibration behavior of FG-Plate. In the beginning, the FG-plate is divided into N-layers along its thickness (N=5 in simulation of experimental work and N=10 in theoretical work) (see Figure 5). Then, the N-plates with dimensions (Length*Width*(thickness/N)) are drawn with zero distance between them (see Figure 8(a)) and then glue them to gather. After that, N-sets of Material properties are interred to ANSYS software (see Figure 8(b)). The element (SOLID187) is used is this model (see Figure 8(c)) to mesh the N-plates (see Figure 8(d)). The adopted boundary conditions and the model analysis are utilized to calculate the natural frequencies of FG-plate [31, 32].

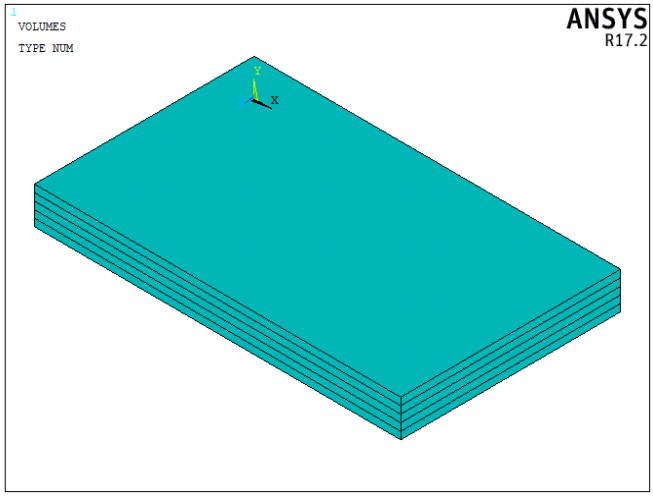

(a) N-plates

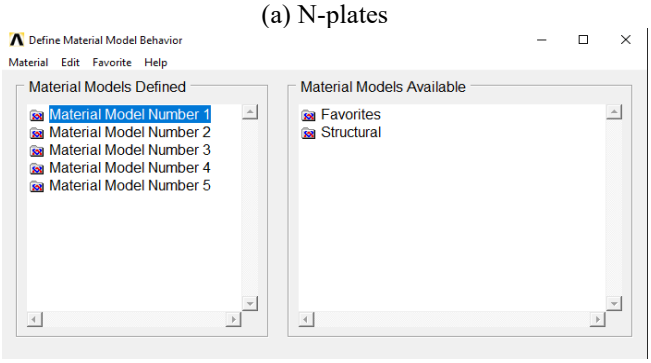

(b) Five sets of material properties

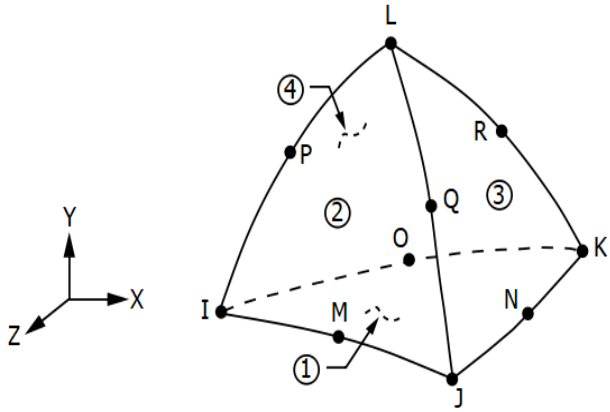

(c) SOLID187

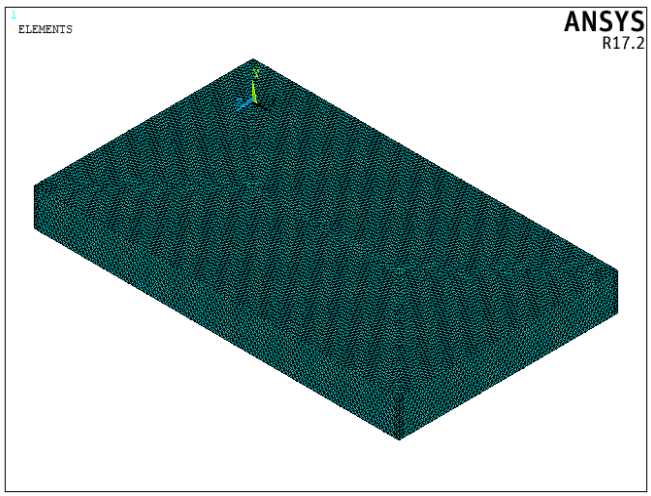

(d) Meshing

Figure 8. ANSYS simulation

4. VALIDATION

4.1 Validation with available literatures

By contrasting the current model's results with the existing literature, the validity of the finite element model is examined in this part. The natural frequencies of the square FG-Plate created by ZrO_2 and Ti-6Al-4V were determined by Bourihane et al. [22] using easily supported boundary conditions.

The 3rd-order shear deformation plate kinematics (TSDT) and classical plate theory (CPT) were employed by Bourihane et al. [22], who then compared their findings with those calculated by Huang and Shen [33]. Table 7 lists the material characteristics of the progenitors of FGM. The plate's dimensions are Length=Width=0.2 m and Thickness=0.025 m. Table 8 shows how the current model compares to findings from Huang and Shen [33] and Bourihane et al. [22]. Table 8 shows that the results of the current model and those of Bourihane et al. [22] coincide quite well (TSDT).

Table 7. Material properties of ZrO_2 and Ti-6Al-4V [22, 26]

Property	Unit	Materials	
		ZrO_2	Ti-6Al-4V
Density	kg/m^3	3000	4429
Young's Modulus	GPa	244.27	122.56
Poisson Ratio	-	0.288	0.31

Table 8. Comparison of natural frequencies for FG-plates made by ZrO_2 and Ti-6Al-4V

Mode	References	FG-Plate				
		ZrO_2 (m=0)	m=1/2	m=1	m=2	Ti-6Al-4V (m=∞)
(1,1)	[33]	8,270	7,130	6,657	6,286	5,400
	[22]-TSDT	8,968	7,530	6,980	6,513	5,228
	[22]-CPT	9,723	8,073	7,429	6,930	5,668
	Present Work (FEM)	8,492.2	7,045.8	6,552.5	6,069.8	4,975.3
(1,2)	[33]	19,261	16,643	15,514	14,625	12,571
	[22]-TSDT	21,276	17,871	16,551	15,413	12,404
	[22]-CPT	24,235	20,093	18,465	17,212	14,128
	Present Work (FEM)	21,276	17,871	16,551	15,413	12,404
(2,2)	[33]	34,870	30,174	28,120	26,454	22,762
	[22]-TSDT	36,342	30,813	28,276	25,850	21,187
	[22]-CPT	36,342	30,827	28,296	25,867	21,187
	Present Work (FEM)	36,342	30,813	28,276	25,850	21,187

4.2 Validation with experimental work

In this section, three FG-plate are made polyester-silica powder and with dimensions (Length=50 cm, Width=13 cm, and Thickness=2 cm) and supporting as CFFF condition. Three values of power-law index are used in experimental work and these values are 1/2, 1 and 5, and Young's modulus of five layers of each FG-plate are listed in Tables 4-6, while, the density $(\rho_{layer\ i})$ and Poisson ratio$(\mu_{layer\ i})$ of each layer are calculated using the following equations:

$$\rho(z) = (\rho_2 - \rho_1)\left(\frac{z}{h} + 0.5\right)^m + \rho_1 \quad (4)$$

$$\rho_{layer\ i} = \frac{(\rho_{point\ i+1} - \rho_{point\ i})}{2} \quad (5)$$

$$\mu(z) = (\mu_2 - \mu_1)\left(\frac{z}{h} + 0.5\right)^m + \mu_1 \quad (6)$$

$$\mu_{layer\ i} = \frac{(\mu_{point\ i+1} - \mu_{point\ i})}{2} \quad (7)$$

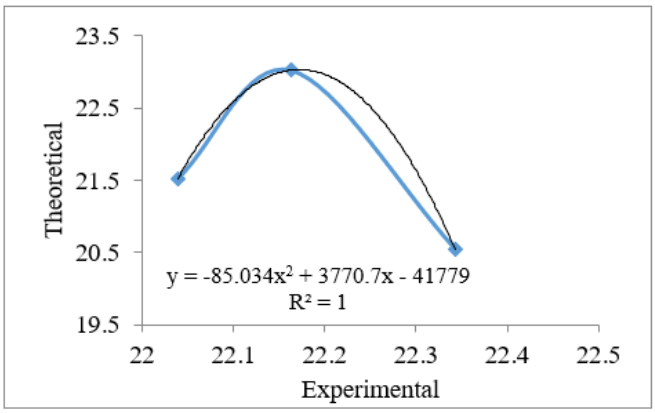

Figure 9. Regression value of natural frequency for the experimental and theoretical FG-plates

Table 9. Fundamental natural frequency comparison of the experimental and theoretical parts for FG-plates made by polyester-silica powder

Power Law Index (m)	Frequency (Hz)		Error (%)
	Experimental	Theoretical	
1/2	20.541	22.343	-8.773
1	23.021	22.163	3.727
5	21.524	22.039	-2.393

A comparison between the experimental and theoretical results is presented in Table 9. One can see that there is a very good agreement between the experimental and theoretical results. The maximum absolute error percentage is (8.773%) when m=1/2. Furthermore, Figure 9 indicate the relationship for natural frequency for FG-plates made by polyester-silica powder for the theoretical FEM and the experimental parts.

5. RESULTS AND DISCUSSION

In this section, the effect of many parameters; power law index, modular ratio, length/thickness, mode number and supporting types, on the natural frequencies of FG-plate are investigated.

5.1 Modular ratio and material index (power law index)

Figure 10 shows the variation of the first fifth natural frequencies of FG-plate that is clamped for four edges (CCCC FG-plate) at different modular ratio (E1/E2) when the length/thickness ratio (L/h) is 5. Generally, one can see that the increase material index more than 5 causes slight variation (increase or decrease) in natural frequencies (first to fifth natural frequencies) for any modular ratio excepted to one. Physically, this happens because the volume fraction of material 2 or top (i.e., $V_2 = \left(\frac{z}{h} + 0.5\right)^m$), approaches to zero and the volume fraction of material (1 or bottom) (V_1=1-V_2) approaches to 1 (see Eq. (2)). For example, the volume fraction of material 2 or top at z=0 is 0.5^m and this value decreases with increasing power law index (m).

When m=1, the linear relationship between V_1 and V_2 appears, (i.e., V_1 increases with decreasing V_2 and vice versa). When m<1, the volume fraction of material 2 or top at z=0 is 0.5^m and this value increases and approaches to 1 with decreasing m and the corresponding value of the volume fraction of material 1 or bottom (V_1=1-V_2) approaches to zero. The values of V_1 and V_2 mean the percentage of materials (1) and (2) in composite FG-plate and these values don't work alone but their effect depends on modular ratio (E1/E2).

When modular ratio equals unity (i.e., the plate contains one material only), the effect of material index vanishes (see Figure10(c)). If E_2 is greater than E_1 (i.e., modular ratio <1), the frequency of FG-plate increases with increase material index because the volume fraction of material 2 decreases and the FG-plate be more stiffened (see Figures 10(a)-(b)). In other side, the stiffness of FG-plate decreases if E_2 is smaller than E_1 (i.e., Modular ratio >1) (see Figures 10(d)-(e)).

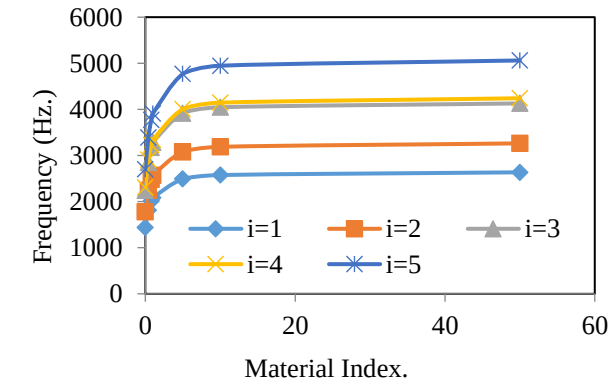

(a) Modulus/Ratio=0.25

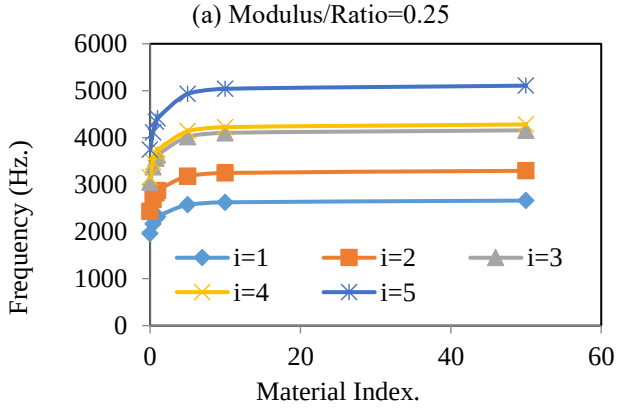

(b) Modulus/Ratio=0.5

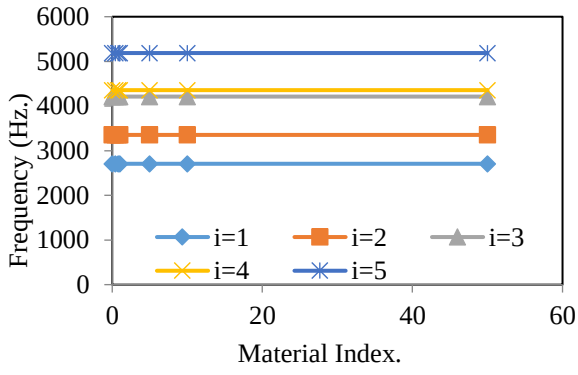

(c) Modulus/Ratio=1

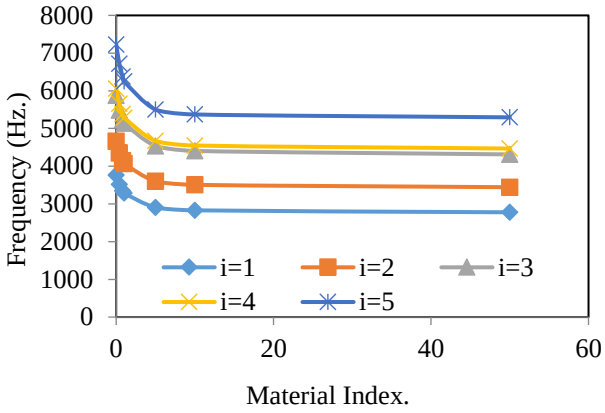

(d) Modulus/Ratio=2

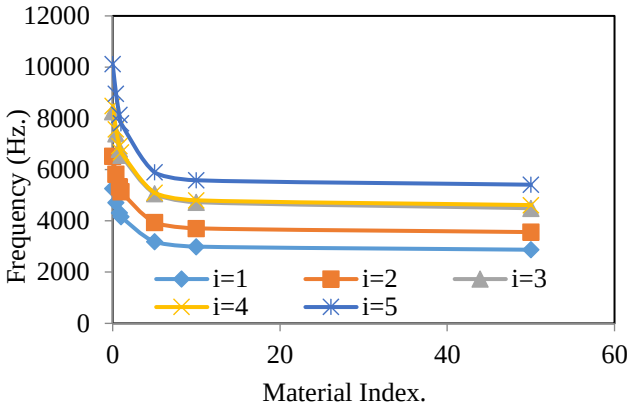

(e) Modulus/Ratio=4

Figure 10. Frequency for CCCC FG-plate due to varying of power law index (m) at different modulus/ratio and L/h=5

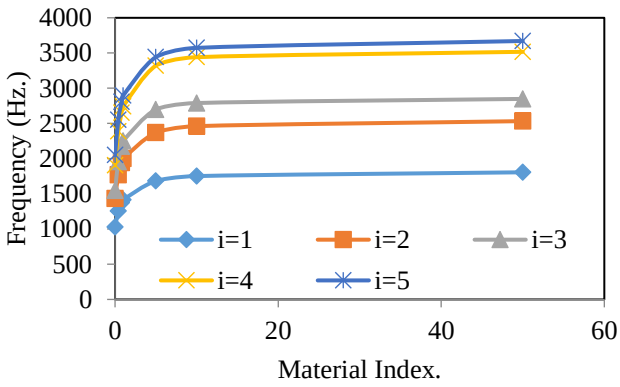

(a) Modulus/Ratio=0.25

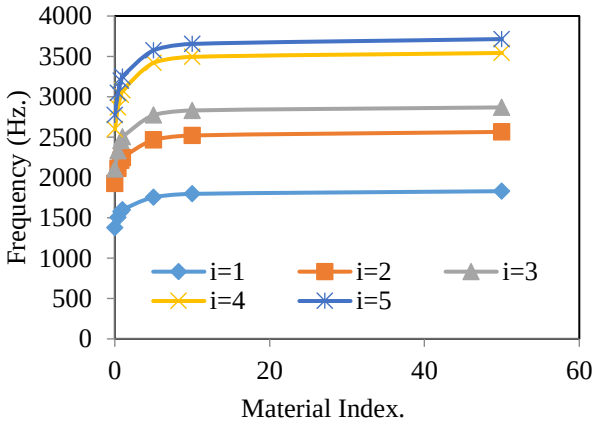

(b) Modulus/Ratio=0.5

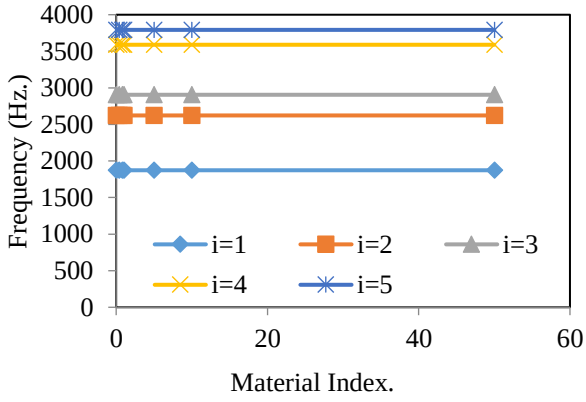

(c) Modulus/Ratio=1

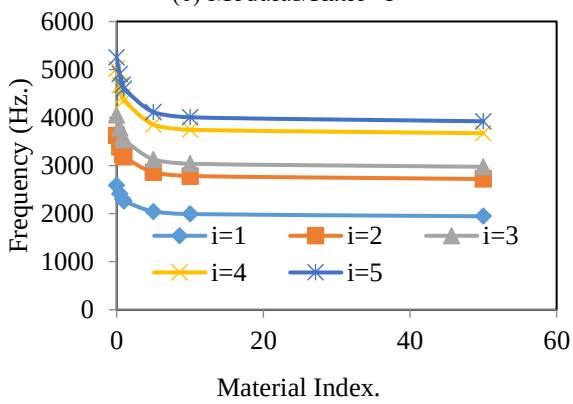

(d) Modulus/Ratio=2

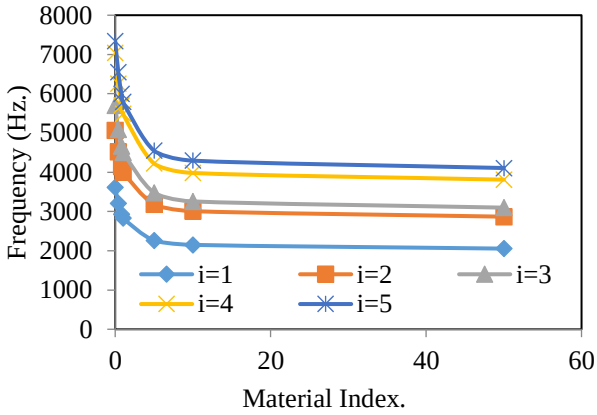

(e) Modulus/Ratio=4

Figure 11. Frequency for SSSS FG-plate due to varying of power law index (m) at different modulus/ratio and L/h=5

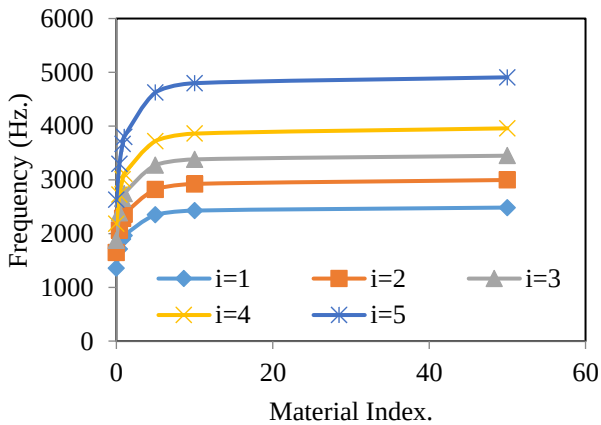

(a) Modulus/Ratio=0.25

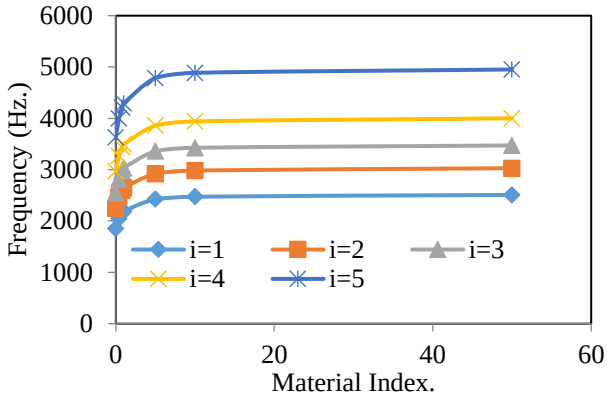

(b) Modulus/Ratio=0.5

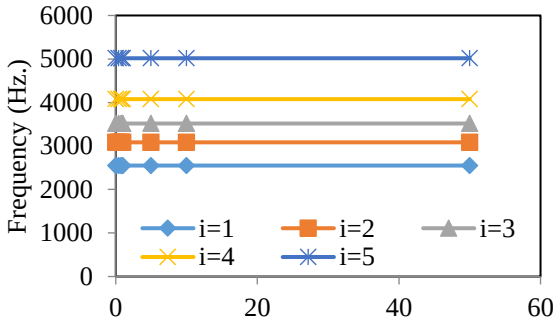

(c) Modulus/Ratio=1

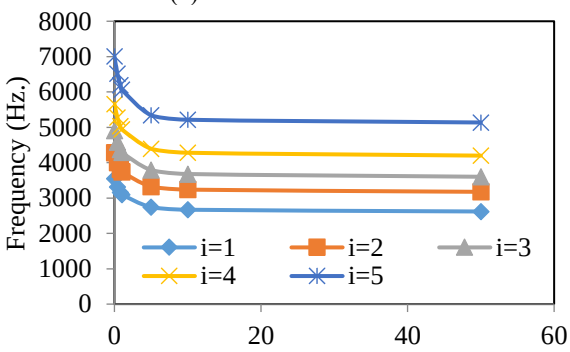

(d) Modulus/Ratio=2

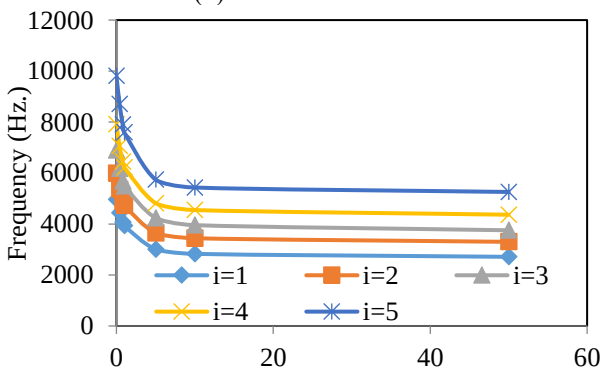

(e) Modulus/Ratio=4

Figure 12. Frequency for SCSC FG-plate due to varying of power law index (m) at different modulus/ratio and L/h=5

Similar variation behavior can be seen for natural frequency of simply supported FG-plate (SSSS FG-plate) and simply-clamped-simply-clamped FG-plate as shown in Figure 11 and Figure 12 respectively. This can mean that higher index results in a softer surface reducing overall stiffness and leading to lower natural frequencies. Also, high modular ratio can be beneficial for aerospace applications needs stiffness tuning to evade unwanted vibrations.

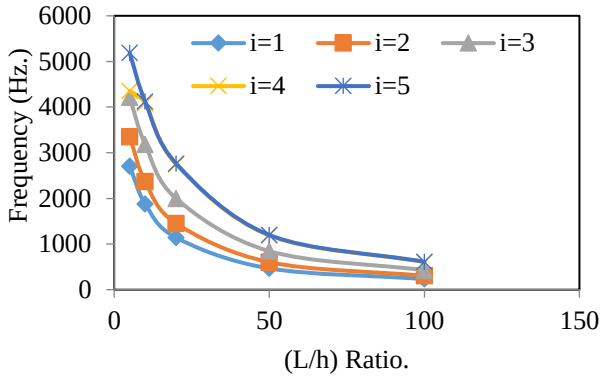

(a) CCCC

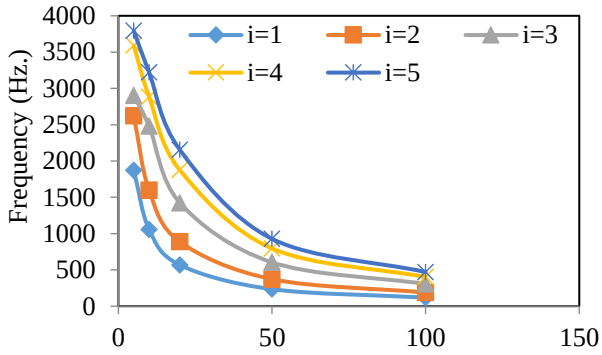

(b) SSSS

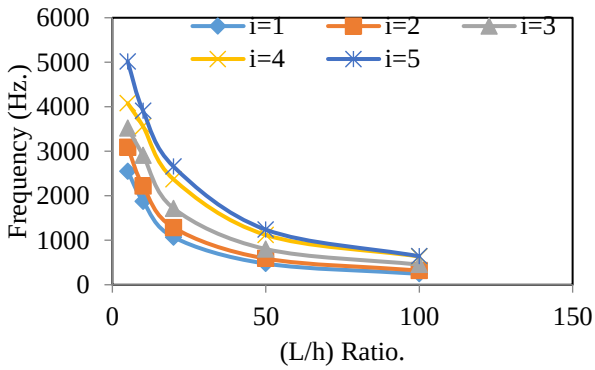

(c) SCSC

Figure 13. First five natural frequencies for FG-plate due to varying of (L/h) ratio at different three supporting type when modulus/ratio =1

5.2 Length/thickness ratio (L/h) and material index

The impact of the L/h ratio on the first five natural frequencies of a homogeneous plate (Modular ratio =1) with varying supporting types is depicted in Figure 13. The material index has no effect on the FG-plate's natural frequency when Modular ratio =1, and the (L/h) ratio has the sole effect. As the (L/h) ratio increases, the natural frequency drop, which is given the same dimensions, material, and supporting type, the natural frequency of thick plates is higher than that of thin plates.

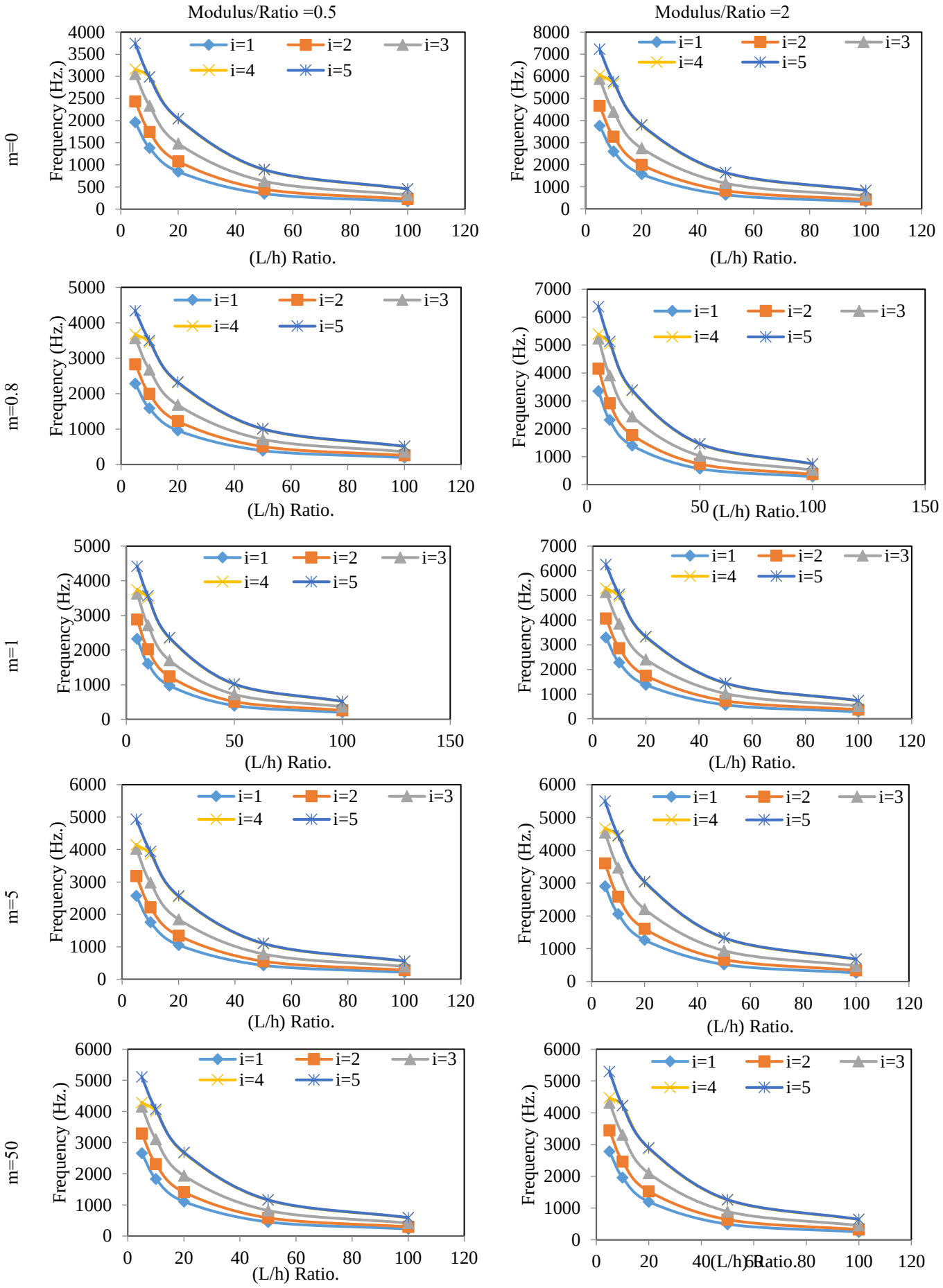

Figure 14. Variation of first five natural frequencies for CCCC FG-plate due to varying of (L/h) ratio at different material index when modulus/ratio=0.5 and 2

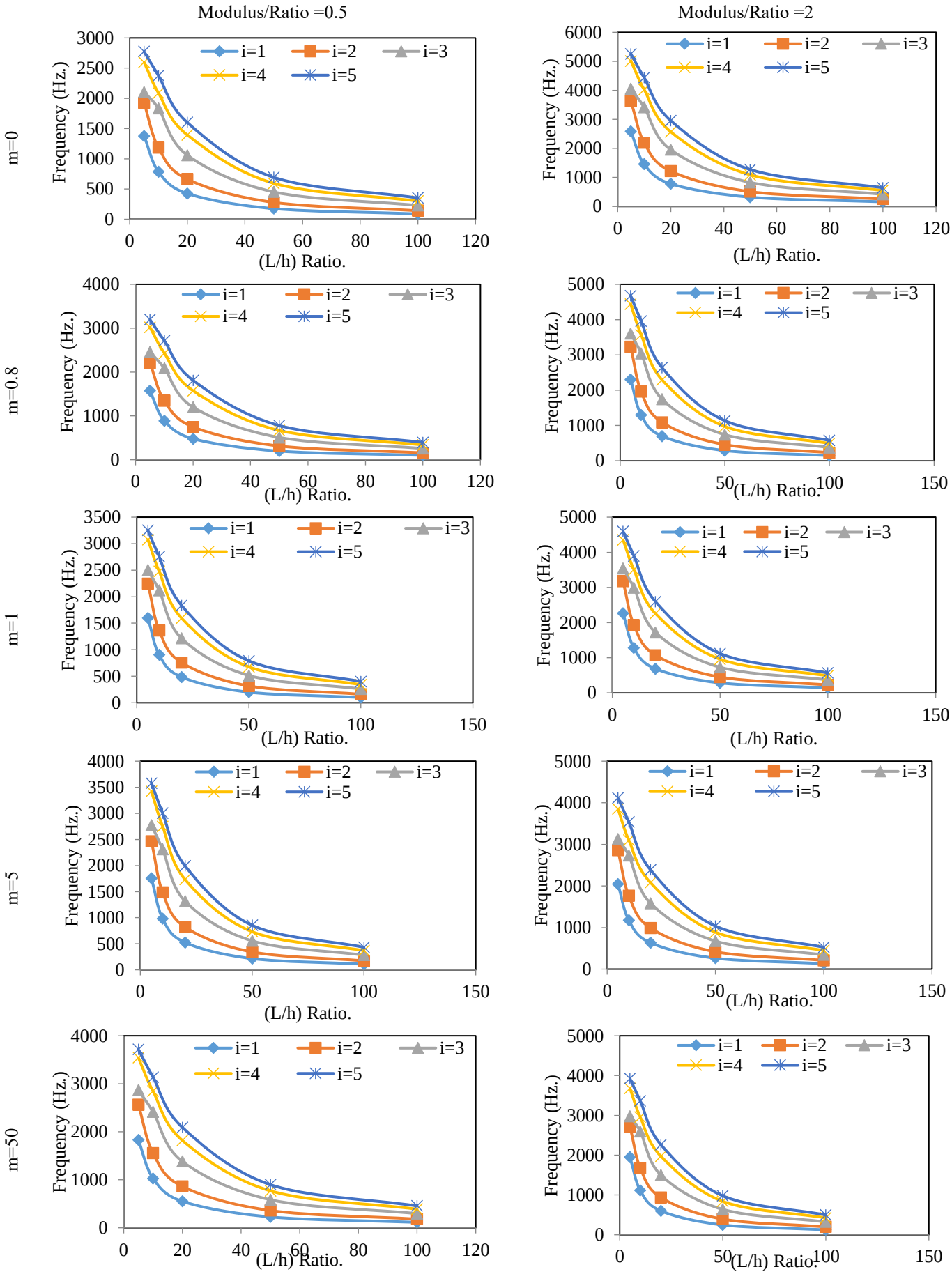

Figure 15. Variation of first five natural frequencies for SSSS FG-plate due to varying of (L/h) ratio at different material index when modulus/ratio=0.5 and 2

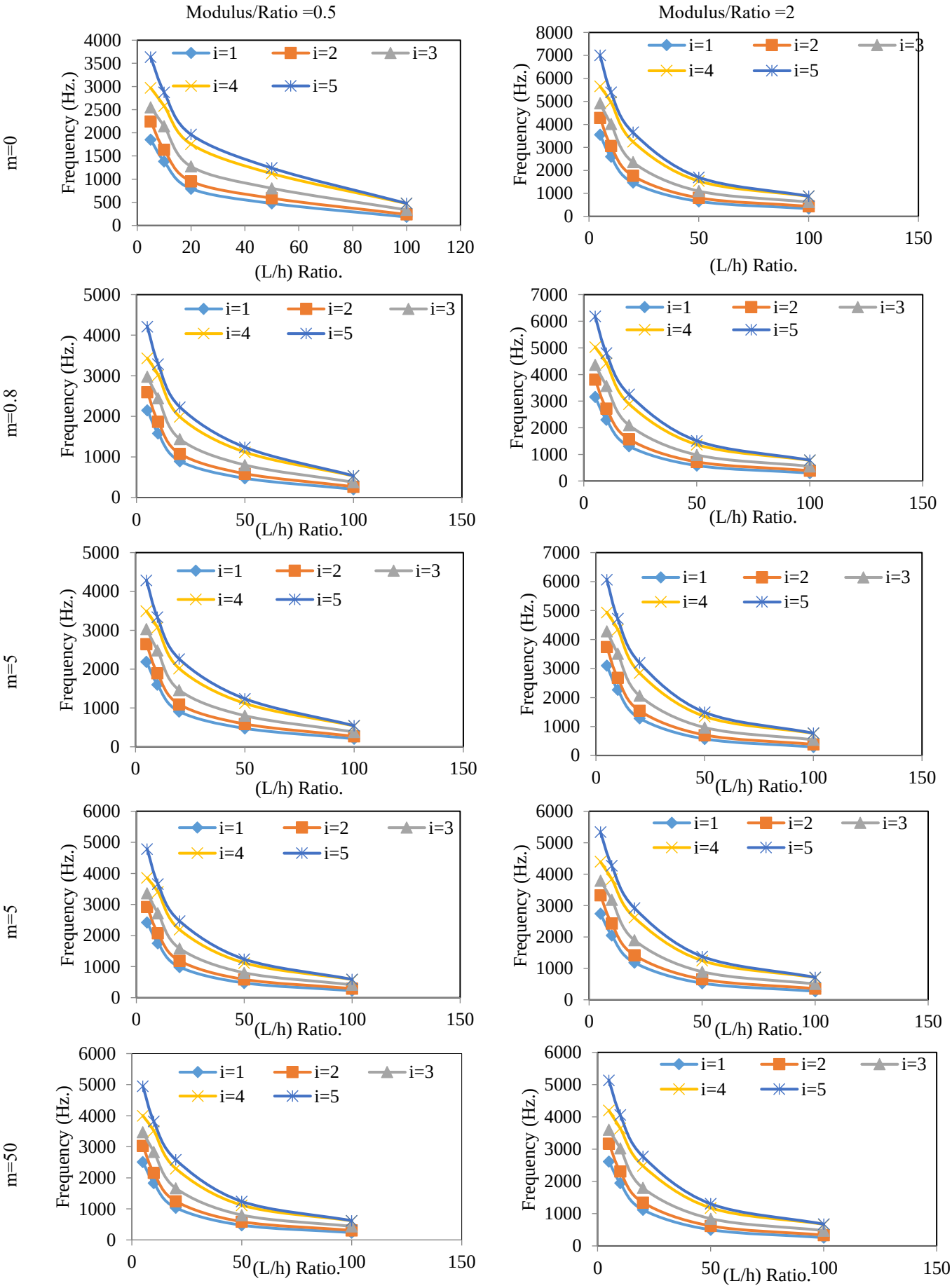

Figure 16. First five natural frequencies for SCSC FG-plate due to varying of (L/h) ratio at different material index when modulus/ratio =0.5 and 2

Generally, the natural frequency increases when the thickness of FG-plate increases and length of FG-plate is constant because increasing of the shear effect. In other side, the shear effect decreases when the thickness of FG-plate decreases and length of FG-plate is constant and this leads to decrease the natural frequency of plate.

For FG-plate, Figures 14-16 illustrate the variation of natural frequencies due to increase (L/h) ratio with different supports CCCC, SSSS and SCSC, respectively.

Figure 14, where modular ratio =1/2 and 2, compares the first five natural frequencies of CCCC FG-plate for various material indices. When m=0, or homogenous material (2), the modular ratio effect manifests, and the (L/h) ratio impact is comparable to that shown in Figure 12(a). The plate goes from thick to thin, allowing one to observe that the natural frequencies fall as the (L/h) ratio increases. The natural frequencies of FG-plate, CCCC, on the other hand, increase as the material index rises when modular ratio =0.5. Modular ratio =2 causes the natural frequencies of FG-plate, CCCC, to decrease as the material index increases. As the (L/h) ratio increases, the natural frequencies for SSSS FG-plate drop because, as Figure 15, the plate transitions from a thick to a thin one. The FG-plate's inherent frequencies also rise when the material index rises when the modular ratio is equal to 0.5. When modular ratio =2, the volume proportion of the two parents (material 1 and material 2) changes, causing the natural frequencies of the FG-plate to decrease as the material index increases. As the plate in Figure 16 changes from a thick to a thin one, the natural frequencies of the SCSC FG-plate decrease as the (L/h) ratio increases. Additionally, the natural frequencies of the SCSC FG-plate increase when the material index increases when the modular ratio equals 1/2. When the modular ratio =2, the natural frequencies of the SCSC FG-plate decrease as the material index increases due to changes in the volume fraction of the two parents (material 1 and material 2).

5.3 Mode number and supporting type

From Figures 10-16, it can be seen that the natural frequency increases with increasing mode number for any material index, modular ratio and supporting type. In other side, the natural frequency of CCCC FG-plate is larger than that of SCSC FG-plate and SSSS FG-plate respectively for the same modular ratio, material index, mode number and L/h ratio. This can lead that for aerospace structures, choosing the boundary constraints is important in controlling vibration and avoiding resonance. On can conclude that clamped plates are preferred in high stiffness and minimal vibration applications, while simply supported configurations may be more suitable for flexible and adaptive structures.

6. CONCLUSIONS AND FUTURE WORKS

This paper presents a novel experimental procedure to fabricate the FG-plates made by polyester resin and silica powder utilizing tensile test results of polyester / silica powder composite materials. The experimental results of vibration test are compared with the finite element method from ANSYS program. The effects of several parameters, modular ratio, material index, (L/h) ratio, and different supporting conditions are investigated. Some of the main findings is that, when the modulus ratio is unity, the material index or power law index is not affected on the natural frequencies. While the natural frequencies decrease with increasing power law when the modulus ratio is exceeds the unity. But the natural frequencies increase with increasing power law when the modulus ratio is smaller than unity. Also, the natural frequencies decreasing with increasing (L/h) ratio. As a future work, using other models of material properties variation such as exponential and sigmoid models are interesting. Also, studying the influences of cracks on the natural frequencies of FG-plates and fabrication FG-plate using powder technology are good research areas.

REFERENCES

[1] Singh, R.K., Rastogi, V. (2021). A review on solid state fabrication methods and property characterization of functionally graded materials. Materials Today: Proceedings, 47: 3930-3935. https://doi.org/10.1016/j.matpr.2021.03.634.

[2] Boggarapu, V., Gujjala, R., Ojha, S., Acharya, S., Chowdary, S., kumar Gara, D. (2021). State of the art in functionally graded materials. Composite Structures, 262: 113596. https://doi.org/10.1016/j.compstruct.2021.113596

[3] Al-Ansari, L.S., Abood, N.K. (2024). Determining numerically the natural frequency of porous functionally graded beam. Kerbala Journal for Engineering Sciences, 4(2).

[4] Al-Hajjar, A.M., Aljassani, A.M., Abdulsamad, H.J., Al-Ansari, L.S. (2024). Investigating static deflection of axial functionally graded non-prismatic beams using the Rayleigh method. Mathematical Modelling of Engineering Problems, 11(7). https://doi.org/10.18280/mmep.110712

[5] Rahmani, F., Kamgar, R., Rahgozar, R. (2022). Optimum material distribution of porous functionally graded plates using Carrera unified formulation based on isogeometric analysis. Mechanics of Advanced Materials and Structures, 29(20): 2927-2941. https://doi.org/10.1080/15376494.2021.1881845

[6] Monajati, L., Farid, N., Farid, M., Parandvar, H. (2022). Vibration and buckling analyses of functionally graded plates based on refined plate theory using airy stress function. Proceedings of the Institution of Mechanical Engineers, Part C: Journal of Mechanical Engineering Science, 236(15): 8231-8244. https://doi.org/10.1177/09544062221087086

[7] Cho, J.R. (2022). Free vibration analysis of functionally graded sandwich plates with a homogeneous core. Applied Sciences, 12(12): 6054. https://doi.org/10.3390/app12126054

[8] Kumar, V., Singh, S.J., Saran, V.H., Harsha, S.P. (2022). Vibration response of exponentially graded plates on elastic foundation using higher-order shear deformation theory. Indian Journal of Engineering and Materials Sciences, 29(2): 181-188, https://doi.org/10.56042/ijems.v29i2.46300

[9] Vel, S.S., Batra, R.C. (2004). Three-dimensional exact solution for the vibration of functionally graded rectangular plates. Journal of Sound and Vibration, 272(3-5): 703-730. https://doi.org/10.1016/S0022-460X(03)00412-7

[10] Altenbach, H., Eremeyev, V.A. (2009). Eigen-vibrations of plates made of functionally graded material. CMC-

Computers, Materials & Continua, 9(2): 153-178. https://doi.org/10.3970/cmc.2009.009.153
[11] Natarajan, S., Baiz, P.M., Bordas, S., Rabczuk, T., Kerfriden, P. (2011). Natural frequencies of cracked functionally graded material plates by the extended finite element method. Composite Structures, 93(11): 3082-3092. https://doi.org/10.1016/j.compstruct.2011.04.007
[12] Janghorban, M., Rostamsowlat, I. (2012). Free vibration analysis of functionally graded plates with multiple circular and non-circular cutouts. Chinese Journal of Mechanical Engineering, 25: 277-284. https://doi.org/10.3901/CJME.2012.02.277
[13] Lei, Z.X., Liew, K.M., Yu, J.L. (2013). Free vibration analysis of functionally graded carbon nanotube-reinforced composite plates using the element-free kp-Ritz method in thermal environment. Composite Structures, 106: 128-138. https://doi.org/10.1016/j.compstruct.2013.06.003
[14] Sharma, A.K., Chauhan, P.S., Narwaria, M., Pankaj, R. (2016). Vibration analysis of functionally graded plates with multiple circular cutouts. International Conference on Futuristic Trends in Engineering, Science, Humanities, and Technology, 2(3): 15-21.
[15] Gupta, A., Talha, M., Chaudhari, V.K. (2016). Natural frequency of functionally graded plates resting on elastic foundation using finite element method. Procedia Technology, 23: 163-170. https://doi.org/10.1016/j.protcy.2016.03.013
[16] Song, M., Kitipornchai, S., Yang, J. (2017). Free and forced vibrations of functionally graded polymer composite plates reinforced with graphene nanoplatelets. Composite Structures, 159: 579-588. https://doi.org/10.1016/j.compstruct.2016.09.070
[17] Ghassabi, A.A. (2017). Free vibration analysis of functionally graded rectangular nano-Plates considering spatial variation of the nonlocal parameter. Master's thesis, Middle East Technical University, Turkey.
[18] Akbaş, Ş.D. (2017). Vibration and static analysis of functionally graded porous plates. Journal of Applied and Computational Mechanics, 3(3): 199-207. https://doi.org/10.22055/JACM.2017.21540.1107
[19] Hien, T.D., Lam, N.N. (2018). Vibration of functionally graded plate resting on viscoelastic elastic foundation subjected to moving loads. IOP Conference Series: Earth and Environmental Science, 143(1): 012024. https://doi.org/10.1088/1755-1315/143/1/012024
[20] Sharma, A.K., Sharma, P., Chauhan, P.S., Bhadoria, S.S. (2018). Study on harmonic analysis of functionally graded plates using FEM. International Journal of Applied Mechanics and Engineering, 23(4). http://doi.org/10.2478/ijame-2018-0053
[21] Nguyen, H.X., Atroshchenko, E., Ngo, T., Nguyen-Xuan, H., Vo, T.P. (2019). Vibration of cracked functionally graded microplates by the strain gradient theory and extended isogeometric analysis. Engineering Structures, 187: 251-266. https://doi.org/10.1016/j.engstruct.2019.02.032
[22] Bourihane, O., Hilali, Y., Mhada, K. (2020). Nonlinear dynamic response of functionally graded material plates using a high-order implicit algorithm. Journal of Applied Mathematics and Mechanics, 100(12): e202000087. https://doi.org/10.1002/zamm.202000087
[23] Hadji, L., Avcar, M. (2021). Free vibration analysis of FG porous sandwich plates under various boundary conditions. Journal of Applied and Computational Mechanics, 7(2): 505-519. https://doi.org/10.22055/jacm.2020.35328.2628
[24] Permoon, M.R., Farsadi, T. (2021). Free vibration of three-layer sandwich plate with viscoelastic core modelled with fractional theory. Mechanics Research Communications, 116: 103766. https://doi.org/10.1016/j.mechrescom.2021.103766
[25] Zaitoun, M.W., Chikh, A., Tounsi, A., Sharif, A., Al-Osta, M.A., Al-Dulaijan, S.U., Al-Zahrani, M.M. (2023). An efficient computational model for vibration behavior of a functionally graded sandwich plate in a hygrothermal environment with viscoelastic foundation effects. Engineering with Computers, 39(2): 1127-1141. https://doi.org/10.1007/s00366-021-01498-1
[26] Narayanan, N.I., Banerjee, S., Kalgutkar, A.P., Rajanna, T. (2021). Vibration analysis of functionally graded material plate. In Recent Advances in Computational Mechanics and Simulations: Volume-I: Materials to Structures. Springer Singapore, pp. 119-130. https://doi.org/10.1007/978-981-15-8138-0_10
[27] Li, D., Deng, Z., Chen, G. (2023). Free vibration of functionally graded sandwich plates in thermal environments. International Journal of Mechanical System Dynamics, 3(1): 39-47. https://doi.org/10.1002/msd2.12063
[28] Vu, V.T., Tran, H.Q. (2024). Free vibration characteristics of stiffened sandwich plates with auxetic core and functionally graded piezoelectric face sheet. Acta Mechanica, 235(6): 4029-4056. https://doi.org/10.1007/s00707-024-03932-z
[29] Hadji, L., Plevris, V., Madan, R., Ait Atmane, H. (2024). Multi-directional functionally graded sandwich plates: Buckling and free vibration analysis with refined plate models under various boundary conditions. Computation, 12(4): 65. https://doi.org/10.3390/computation12040065
[30] Vasiliev, V.V., Morozov, E.V. (2013). Advanced Mechanics of Composite Materials and Structural Elements. Elsevier Ltd. https://doi.org/10.1016/C2011-0-07135-1
[31] Gburi, F.H., Al-Ansari, L.S., Khadom, M.A., Al-Saffar, A.A. (2020). Free vibration of skew isotropic plate using ANSYS. Journal of Mechanical Engineering Research and Developments, 43(5): 472-486.
[32] Neamah, R.A., Shukur, Z.M., Al-Ansari, L.S., Dearn, K.D. (2020). Studying the effect of fiber orientation and skew angle on the fundamental frequencies of simply supported composite plates using finite element method. Journal of Mechanical Engineering Research and Developments, 43: 199-212.
[33] Huang, X.L., Shen, H.S. (2004). Nonlinear vibration and dynamic response of functionally graded plates in thermal environments. International Journal of Solids and Structures, 41(9-10): 2403-2427. https://doi.org/10.1016/j.ijsolstr.2003.11.012